

# $\alpha$ -RuCl<sub>3</sub>: a Spin-Orbit Assisted Mott Insulator on a Honeycomb Lattice

K. W. Plumb,<sup>1</sup> J. P. Clancy,<sup>1</sup> L. J. Sandilands,<sup>1</sup> V. Vijay Shankar,<sup>1</sup>  
Y.F. Hu,<sup>2</sup> K. S. Burch,<sup>1,3</sup> Hae-Young Kee,<sup>4,5</sup> and Young-June Kim<sup>4,\*</sup>

<sup>1</sup>*Department of Physics and Center for Quantum Materials,  
University of Toronto, 60 St. George St., Toronto, Ontario, M5S 1A7, Canada*

<sup>2</sup>*Canadian Light Source, Saskatoon, Saskatchewan, S7N 0X4, Canada*

<sup>3</sup>*Department of Physics, Boston College, Chestnut Hill, Massachusetts 02467, USA*

<sup>4</sup>*Department of Physics and Center for Quantum Materials,  
University of Toronto, 60 St. George St., Toronto, Ontario, M5S 1A7, Canada*

<sup>5</sup>*Canadian Institute for Advanced Research, Toronto, Ontario, M5G 1Z8, Canada*

(Dated: March 19, 2014)

We examine the role of spin-orbit coupling in the electronic structure of  $\alpha$ -RuCl<sub>3</sub>, in which Ru ions in 4d<sup>5</sup> configuration form a honeycomb lattice. The measured optical spectra exhibit an optical gap of 220 meV and transitions within the t<sub>2g</sub> orbitals. The spectra can be described very well with first-principles electronic structure calculations obtained by taking into account both spin-orbit coupling and electron correlations. Furthermore, our x-ray absorption spectroscopy measurements at the Ru L edges exhibit distinct spectral features associated with the presence of substantial spin-orbit coupling, as well as an anomalously large branching ratio. We propose that  $\alpha$ -RuCl<sub>3</sub> is a spin-orbit assisted Mott insulator, and that the bond-dependent Kitaev interaction may be relevant for this compound.

PACS numbers: 75.10.Jm, 71.20.Be, 71.70.Ej, 78.70.Dm

Novel electronic ground states can often result from the interplay of many competing energy scales. In magnetic materials containing 4d and 5d transition metals, the combination of electronic correlations and spin-orbit coupling (SOC) can give rise to exotic topological phases [1–11]. When a transition metal ion is subject to an octahedral crystal field environment, SOC mixes the wave functions of the triply-degenerate t<sub>2g</sub> electronic states and the low energy magnetic degrees of freedom are described by spin-orbital mixed Kramers doublets, termed  $J_{\text{eff}}$  states [6, 7]. One of many interesting consequences of  $J_{\text{eff}}$  states in real materials is the presence of an unusual bond-dependent exchange term called the Kitaev interaction. This bond-dependent interaction is a crucial ingredient for realizing a quantum spin liquid phase on a honeycomb lattice [1, 7, 12]. Thus far, large efforts have been directed towards studying the 5d A<sub>2</sub>IrO<sub>3</sub> (A=Na or Li) compounds where IrO<sub>6</sub> octahedra share edges to form a honeycomb network [13–19]. The edge-sharing geometry suppresses isotropic Heisenberg interactions while Kitaev interactions are believed to be substantial [6, 7]. However, due to monoclinic and trigonal distortions, the applicability of the localized  $J_{\text{eff}}$  picture to these compounds is still controversial [20, 21]. In light of this complication it would be extremely useful to search for a system which is free of these distortions in which to study spin-orbit driven physics.

The 4d counterpart of iridate physics can be found in Ru<sup>3+</sup> (4d<sup>5</sup>) compounds. Even though the absolute value of SOC in 4d systems is smaller than that of 5d elements, the spin-orbital mixed state may still be realized as long as the t<sub>2g</sub> states remain degenerate in the absence of SOC [22].  $\alpha$ -RuCl<sub>3</sub> is an insulating transition metal

halide with honeycomb layers composed of nearly ideal edge-sharing RuCl<sub>6</sub> octahedra. While earlier transport measurements have implicated  $\alpha$ -RuCl<sub>3</sub> to be a conventional semiconductor [23], subsequent spectroscopic investigations suggest that it may be a Mott insulator [24]. Owing to the near ideal edge-sharing honeycomb geometry and the insulating behaviour,  $\alpha$ -RuCl<sub>3</sub> is potentially an excellent candidate material in which to realize Kitaev physics. However, the microscopic origin of such an insulating state in  $\alpha$ -RuCl<sub>3</sub> remains poorly understood and a systematic investigation of the role of SOC in this material has not been conducted until now.

In this Letter, we show that the insulating state in  $\alpha$ -RuCl<sub>3</sub> arises from the combined effects of electronic correlations and strong SOC. In order to probe the detailed electronic structure of  $\alpha$ -RuCl<sub>3</sub>, we have carried out optical spectroscopy measurements. The origins of the optical gap in  $\alpha$ -RuCl<sub>3</sub> are elucidated by our band structure calculations. We find that while strong electronic correlations are necessary to describe this material, SOC is essential to account for the magnitude of the optical gap. Furthermore, we have performed x-ray absorption spectroscopy (XAS) measurements which directly indicate substantial SOC of 4d electrons. Taken as a whole, our results indicate that  $\alpha$ -RuCl<sub>3</sub> is best described as a spin-orbit assisted Mott insulator and strong SOC effects must be considered to understand this material.

The crystal structure of  $\alpha$ -RuCl<sub>3</sub> is shown in Fig. 1. Edge sharing RuCl<sub>6</sub> octahedra form a honeycomb network in the a-b plane and the weakly coupled honeycomb layers are stacked along the c-direction to form a CrCl<sub>3</sub> type structure  $P3_112$  [26]. As shown in Fig. 1 (c), the

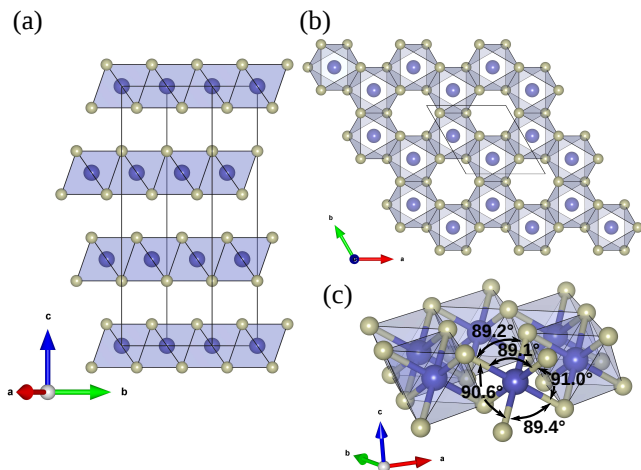


FIG. 1: (Color online) (a) The crystal structure of  $\alpha$ - $\text{RuCl}_3$ , exhibiting lamellar nature of the unit cell. (b) Individual honeycomb layers are formed by edge-sharing  $\text{RuCl}_6$  octahedra (Ru in blue, Cl in grey). (c) Detailed view of  $\text{RuCl}_6$  octahedra showing bond angles. All the figures were produced with VESTA [25].

Cl-Ru-Cl angles are all within  $1^\circ$  of  $90^\circ$  and the Ru-Cl bond lengths are within 0.3% of one another. Thus, the  $\text{RuCl}_6$  octahedron in this compound is very close to ideal. In fact, the absence of appreciable electric quadrupole interactions from the  $^{99}\text{Ru}$  Mössbauer spectroscopy study was interpreted to result from the highly symmetric octahedral configuration of the ligand Cl ions [27]. This structural detail is quite important since such an ideal octahedral environment will leave the  $t_{2g}$  states degenerate in the absence of SOC. In contrast,  $\text{Na}_2\text{IrO}_3$  has an O-Ir-O bond angle of about  $85^\circ$  [16, 17]. Another important structural difference between  $\text{Na}_2\text{IrO}_3$  and  $\alpha$ - $\text{RuCl}_3$  is the lack of intervening Na atoms between the honeycomb layers in the latter compound, such that  $\alpha$ - $\text{RuCl}_3$  is closer to an ideal two-dimensional system.

Single crystal samples of  $\alpha$ - $\text{RuCl}_3$  were prepared by vacuum sublimation from commercial  $\text{RuCl}_3$  powder. The dielectric function  $\hat{\epsilon}(\omega) = \epsilon_1(\omega) + i\epsilon_2(\omega)$  of  $\text{RuCl}_3$  was measured from 0.1 to 6 eV; for the range 0.9 to 6 eV,  $\hat{\epsilon}(\omega)$  was determined using spectroscopic ellipsometry. From 0.1 to 1.2 eV, we measured the transmittance through a thin  $\text{RuCl}_3$  sample and extracted  $\hat{\epsilon}(\omega)$  using a standard model for the transmittance of a plate sample [28]. X-ray absorption spectroscopy measurements were performed using the Soft x-ray Microcharacterization Beamline (SXRMB) at the Canadian Light Source. Measurements were carried out at the Ru  $L_3$  ( $2p_{3/2} \rightarrow 4d$ ) and  $L_2$  ( $2p_{1/2} \rightarrow 4d$ ) absorption edges. More details of the experimental procedure are contained in the Supplemental Material.

Physical properties of  $\alpha$ - $\text{RuCl}_3$  have been extensively investigated. The magnetic susceptibility of  $\alpha$ - $\text{RuCl}_3$  shows a sharp cusp around 13-15 K, which was attributed

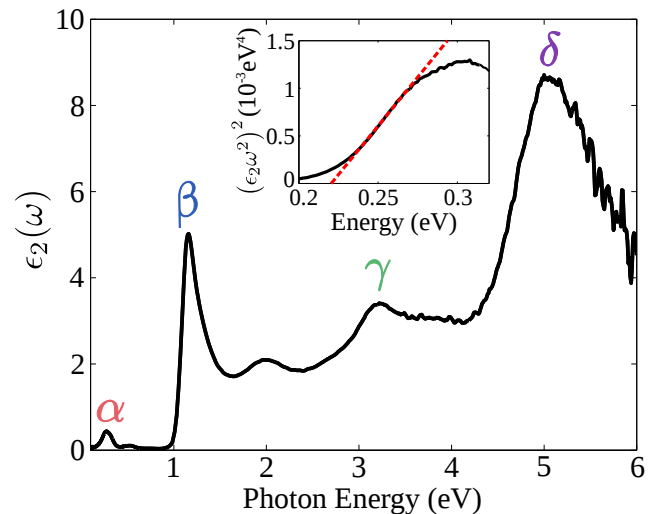


FIG. 2: Imaginary component of the dielectric function  $\epsilon_2(\omega)$  of  $\text{RuCl}_3$  measured at 295 K. The spectrum displays three types of excitations: transitions between  $t_{2g}$  states in the region from 0 to 1 eV;  $t_{2g} \rightarrow e_g$  transitions spanning 1 to 4 eV; and charge transfer excitations in the range of 4 to 6 eV. The peak locations and intensities, as well as the optical gap size, are in good agreement with the LDA+SOC+U band structure. The transitions corresponding to the features labelled  $\alpha$ ,  $\beta$ , and  $\delta$  are shown in figure 3 (a). Inset:  $(\epsilon_2\omega^2)^2$  vs. photon energy in region I; the linear onset indicates an optical gap of  $\approx 220$  meV.

to antiferromagnetic ordering [29]; and a Curie-Weiss fit yields effective local moment of about  $2.2 \mu_B$  and ferromagnetic Curie-Weiss temperature of 23-40 K [27, 29]. The effective magnetic moment is much larger than the spin only value of  $1.73 \mu_B$  for the low spin ( $S=1/2$ ) state of  $\text{Ru}^{3+}$ , indicating a significant orbital contribution to total moment. Based on these observations, it was suggested that the nearest neighbor interaction within the honeycomb plane is ferromagnetic and that these planes are weakly coupled with an antiferromagnetic interaction. However, powder neutron diffraction failed to observe magnetic Bragg peaks of (003) type, which are expected from the predicted simple magnetic structure [29]. Although several spectroscopic and transport investigations have been carried out to study the electronic structure of  $\alpha$ - $\text{RuCl}_3$  [23, 24, 30, 31], the role of SOC was not explored in detail in these earlier studies.

In order to better understand the insulating behavior of  $\alpha$ - $\text{RuCl}_3$ , we have conducted optical spectroscopy measurements. In Fig. 2 we show the measured imaginary component of the dielectric function,  $\epsilon_2(\omega)$ . We find no evidence of free carrier absorption which confirms the insulating character of  $\text{RuCl}_3$ . The spectrum can be divided into three regions: i) a series of weak transitions in the range 0.1 to 1 eV, ii) three stronger features located near 1.2, 2 and 3.2 eV, and iii) an intense band centered near 5 eV, in agreement with previous reports [23, 30].

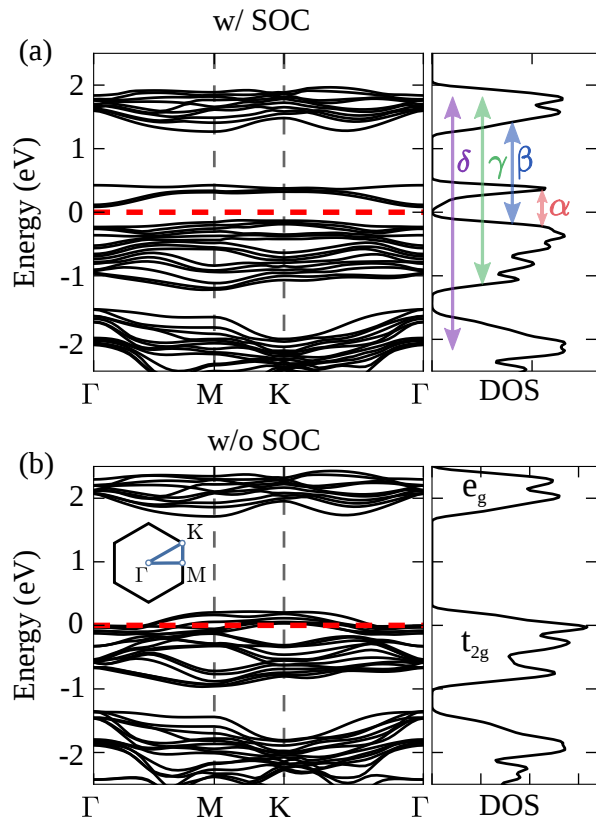


FIG. 3: (Color online) (a) LDA + U + SOC band structure and density of states (DOS) of  $\alpha$ -RuCl<sub>3</sub> along in plane high symmetry points of the BZ ( $k_z=0$ ) with  $U=1.5$  eV and  $J_H=0.3$  eV. Top panel is obtained with SOC and the bottom panel is without the SOC. Optical transitions denoted with arrows and labels using the same notation as in Fig. 2.

Representative features are labeled  $\alpha$ ,  $\beta$  and  $\delta$  as shown in figure 2 to facilitate a comparison with the band structure calculation. Based on a linear onset in the quantity  $(\epsilon_2\omega^2)^2$ , shown in the inset of Fig. 2, we can also identify an optical gap of roughly 220 meV at 295 K [32].

The role of electronic correlations and SOC in generating the optical spectra can be understood from our electronic structure calculations. The band structure and total density of states (DOS) for  $\alpha$ -RuCl<sub>3</sub> were obtained by performing first principles calculations including SOC and are plotted in Fig. 3. Details of the calculation can be found the Supplemental Material. In Fig. 3 (a), we show the band structure and DOS obtained with Hubbard  $U = 1.5$  eV and Hund's coupling  $J_H=0.3$  eV in the presence of SOC. The strength of electron correlation  $U = 1.5$  eV was determined by comparing the direct charge gap with the measured optical gap. The Hund's coupling was chosen to be about 20% of  $U$ , which is typical for 3d or 4d transition metal compounds. On the other hand, Fig. 3 (b) presents the case with the same  $U$  and  $J_H$  strengths as in Fig. 3(a), but in the absence of the SOC. For both cases, one can see clearly the  $t_{2g}$

and  $e_g$  crystal field splitting due to the octahedral environment. However, the key difference is that Fig. 3(a) shows an insulating phase with an unambiguous charge gap, while the band structure is metallic when the SOC is absent as shown in Fig. 3(b). To obtain an insulating state without SOC, a Hubbard  $U$  value greater than 2.5 eV is required. This in turn produces a much larger value for the charge gap which is constrained by the measured optical gap. Therefore, a reasonable description of the insulating phase in  $\alpha$ -RuCl<sub>3</sub> is only possible through the combination of SOC and electron correlation.

Our LDA+U+SOC band structure also agrees well with the optical spectra at higher energies. The  $\alpha$  peak, together with the other weak features below 1 eV, can be understood as transitions between  $t_{2g}$  states. We assign the  $\beta$  feature to the lowest energetically allowed transition between the  $t_{2g}$  and  $e_g$  states as represented by the arrow in Fig. 3(a); the features at 2 and 3.2 eV (labelled  $\gamma$ ) also involve this combination of initial and final states. Finally, we interpret the strong peak near 5 eV (feature  $\delta$ ) as due to transitions from the band 2 eV below the Fermi level to the  $e_g$  states. Indeed, our DFT calculations suggests the band at -2 eV has an increased Cl  $p$  content, meaning the  $\delta$  transition has a charge transfer character. Overall, our optical spectroscopy measurements and electronic structure calculations agree well, and thus identify  $\alpha$ -RuCl<sub>3</sub> as a spin-orbit assisted Mott insulator.

We have independently confirmed the importance of SOC in the electronic structure of  $\alpha$ -RuCl<sub>3</sub> through XAS measurements. The x-ray absorption spectra obtained at the Ru  $L_2$  and  $L_3$  edges are shown in Fig. 4. Two peaks are observed for the  $L_3$  edge data shown in Fig. 4 (a), corresponding to exciting  $2p_{3/2}$  core electron into empty  $t_{2g}$  and  $e_g$  states. The intensity ratio between these two features is related to the fact that there is only one empty  $t_{2g}$  state available for the transition compared to four empty  $e_g$  states. A quantitative description of the intensity and the peak splitting requires ligand field multiplet calculations and is beyond the scope of this letter. Here we instead focus on the different lineshapes observed near the Ru  $L_2$  edge compared to that of the  $L_3$  edge. In particular, the lower energy shoulder corresponding to the transition to the  $t_{2g}$  state is absent for the  $L_2$  edge data. The different lineshapes arise from SOC in the 4d electronic states. At the  $L_2$  ( $2p_{1/2}$ ) edge, the atomic dipole transition  $2p_{1/2} \rightarrow 4d_{3/2}$  is allowed, while the  $J$  selection rule forbids the  $2p_{1/2} \rightarrow 4d_{5/2}$  transition. This is different from the  $L_3$  edge case, in which both  $2p_{3/2} \rightarrow 4d_{3/2}$  and  $2p_{3/2} \rightarrow 4d_{5/2}$  transitions are dipole allowed. The absence of the  $L_2$  peak indicates that the empty  $t_{2g}$  state takes on  $J = 5/2$  character; a result of significant SOC effects. The fact that the lineshape depends crucially on the 4d SOC was first noted by Sham *et al.* in their study of Ru(NH<sub>3</sub>)<sub>6</sub>Cl<sub>6</sub> [33], and later confirmed quantitatively in the multiplet calculation carried out by de Groot *et al.* [34].

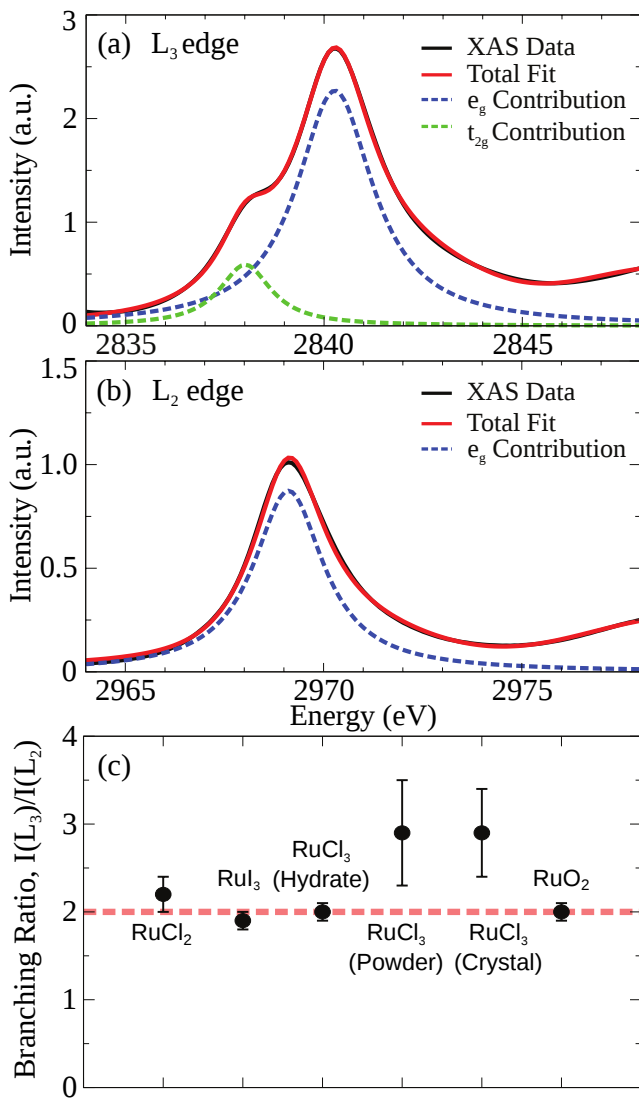


FIG. 4: (Color online) (a) X-ray absorption near edge spectra of RuCl<sub>3</sub> measured at the Ru L<sub>3</sub> edge. The black solid line is the experimental data, and the red solid line is a fit function that includes two Lorentzian peaks associated with t<sub>2g</sub> and e<sub>g</sub> states and an arctan function describing the edge jump. (b) Same spectra showing the energy range of the Ru L<sub>2</sub> edge. The scale is exactly half of the one shown in (a), emphasizing the departure from statistical branching ratio of 2. (c) Comparison of the branching ratio with various Ru standard compounds, ranging from Ru<sup>2+</sup> (RuCl<sub>2</sub>), Ru<sup>3+</sup> (RuI<sub>3</sub>), to Ru<sup>4+</sup> (RuO<sub>2</sub>). Note that RuCl<sub>3</sub> (hydrate) has a structure different from α-RuCl<sub>3</sub> studied here.

Another quantity often used to illustrate the strength of SOC is the so-called branching ratio, defined as the main peak (‘white line’) intensity ratio between the L<sub>3</sub> and L<sub>2</sub> absorption features. Typically, this value is about two. However, when the d-electron SOC is significant, anomalously larger values have been observed; for example, many iridate compounds show large branching ratios [35]. If we take both peaks in the L<sub>3</sub> edge data into ac-

count, the branching ratio of α-RuCl<sub>3</sub> is also quite large:  $3.0 \pm 0.5$ . In Fig. 4 (c), the observed branching ratios for several Ru containing compounds are compared. Clearly α-RuCl<sub>3</sub> exhibits an anomalously large value. Thus, both the lineshape and the branching ratio indicate that the SOC in α-RuCl<sub>3</sub> is substantial.

The perceived similarities of both the crystal and electronic structure between Na<sub>2</sub>IrO<sub>3</sub> and α-RuCl<sub>3</sub> naturally raises questions regarding the relevance of the Kitaev model to α-RuCl<sub>3</sub>. As mentioned earlier, Na<sub>2</sub>IrO<sub>3</sub> is under intense scrutiny due to the possibility of realizing a Kitaev spin liquid phase [1, 5, 7, 10, 11, 13–19, 36–38]. However, the trigonal distortion present in Na<sub>2</sub>IrO<sub>3</sub> brings the atomic basis of the spin-orbit coupled J<sub>eff</sub>=1/2 states into question [20, 21]. Furthermore, Na atoms may promote non-negligible further neighbor exchange terms additional to the nearest neighbor terms [38, 39]. α-RuCl<sub>3</sub> is free from such complexity as it is close to the ideal two-dimensional honeycomb lattice. Even though the atomic SOC is weaker, the ratio of the SOC and the electronic bandwidth is only slightly smaller than in Na<sub>2</sub>IrO<sub>3</sub> because both are reduced in α-RuCl<sub>3</sub> compared to iridates. Indeed we find the bandwidth of α-RuCl<sub>3</sub> to be about half of that in Na<sub>2</sub>IrO<sub>3</sub>, while the SOC is smaller by a factor of ~3. More detailed electronic structure calculations have found that the bands near the Fermi level in α-RuCl<sub>3</sub> are mostly composed of J<sub>eff</sub>=1/2 except in the region near the Γ point [40]; this situation is similar to perovskite iridates [41, 42]. Another important difference between Na<sub>2</sub>IrO<sub>3</sub> and α-RuCl<sub>3</sub> is the large size of Cl anions which expands the lattice; the Ru-Ru distance is about 10% larger than the Ir-Ir distance in Na<sub>2</sub>IrO<sub>3</sub>. As a result, the direct hopping between the Ru t<sub>2g</sub> orbitals is suppressed, and indirect hopping through Cl, which gives rise to a Kitaev interaction, is the most dominant hopping process in α-RuCl<sub>3</sub>. Then a microscopic spin model relevant for α-RuCl<sub>3</sub> should be composed of both the nearest neighbor Heisenberg and bond-dependent exchange terms denoted by Kitaev K and Γ [43–45].

In conclusion, we have carried out combined optical spectroscopy, electronic structure calculations, and x-ray absorption spectroscopy investigation of the role of spin-orbit coupling in α-RuCl<sub>3</sub>. We find that both spin-orbit coupling and electron correlations are necessary to produce an electronic structure consistent with the observed optical gap of about 220 meV. In addition, the calculated electronic structure agrees with measured higher energy optical transitions. Our x-ray absorption spectra clearly illustrate that spin-orbit coupling of the 4d electron system in this compound is significant. Thus spin-orbit coupling plays an essential role in the microscopic magnetic Hamiltonian, and α-RuCl<sub>3</sub> is likely to exhibit unconventional magnetic ordering arising from bond-dependent exchange interactions which could be investigated in future studies.

Research at the University of Toronto was supported by the NSERC, CFI, OMRI, and Canada Research Chair program. Computations were performed on the gpc supercomputer at the SciNet HPC Consortium [46]. SciNet is funded by: the Canada Foundation for Innovation under the auspices of Compute Canada; the Government of Ontario; Ontario Research Fund - Research Excellence; and the University of Toronto. Research described in this paper was performed at the Canadian Light Source, which is funded by the Canada Foundation for Innovation, the Natural Sciences and Engineering Research Council of Canada, the National Research Council Canada, the Canadian Institutes of Health Research, the Government of Saskatchewan, Western Economic Diversification Canada, and the University of Saskatchewan.

---

\* Electronic address: yjkim@physics.utoronto.ca

- [1] A. Kitaev, *Annals of Physics* **321**, 2 (2006).
- [2] X. Wan, A. M. Turner, A. Vishwanath, and S. Y. Savrasov, *Phys. Rev. B* **83** (2011).
- [3] Y. Okamoto, M. Nohara, H. Aruga-Katori, and H. Takagi, *Phys. Rev. Lett.* **99**, 137207 (2007).
- [4] M. J. Lawler, A. Paramakanti, Y. B. Kim, and L. Balents, *Phys. Rev. Lett.* **101**, 197202 (2008).
- [5] A. Shitade, H. Katsura, J. Kuneš, X.-L. Qi, S.-C. Zhang, and N. Nagaosa, *Phys. Rev. Lett.* **102**, 256403 (2009).
- [6] G. Jackeli and G. Khaliullin, *Phys. Rev. Lett.* **102**, 017205 (2009).
- [7] J. Chaloupka, G. Jackeli, and G. Khaliullin, *Phys. Rev. Lett.* **105**, 027204 (2010).
- [8] D. Pesin and L. Balents, *Nat. Phys.* **6**, 376 (2010).
- [9] W. Witczak-Krempa and Y. B. Kim, *Phys. Rev. B* **85** (2012).
- [10] J. Reuther, R. Thomale, and S. Trebst, *Phys. Rev. B* **84**, 100406 (2011).
- [11] F. Trouselet, G. Khaliullin, and P. Horsch, *Phys. Rev. B* **84**, 054409 (2011).
- [12] M. K. Crawford, M. A. Subramanian, R. L. Harlow, J. A. Fernandez-Baca, Z. R. Wang, and D. C. Johnston, *Phys. Rev. B* **49**, 9198 (1994).
- [13] Y. Singh and P. Gegenwart, *Phys. Rev. B* **82**, 064412 (2010).
- [14] X. Liu, T. Berlijn, W.-G. Yin, W. Ku, A. Tsvelik, Y.-J. Kim, H. Gretarsson, Y. Singh, P. Gegenwart, and J. P. Hill, *Phys. Rev. B* **83**, 220403 (2011).
- [15] Y. Singh, S. Manni, J. Reuther, T. Berlijn, R. Thomale, W. Ku, S. Trebst, and P. Gegenwart, *Phys. Rev. Lett.* **108**, 127203 (2012).
- [16] S. K. Choi, R. Coldea, A. N. Kolmogorov, T. Lancaster, I. I. Mazin, S. J. Blundell, P. G. Radaelli, Y. Singh, P. Gegenwart, K. R. Choi, et al., *Phys. Rev. Lett.* **108**, 127204 (2012).
- [17] F. Ye, S. Chi, H. Cao, B. C. Chakoumakos, J. A. Fernandez-Baca, R. Custelcean, T. F. Qi, O. B. Korneta, and G. Cao, *Phys. Rev. B* **85**, 180403 (2012).
- [18] R. Comin, G. Levy, B. Ludbrook, Z.-H. Zhu, C. N. Venstra, J. A. Rosen, Y. Singh, P. Gegenwart, D. Stricker, J. N. Hancock, et al., *Phys. Rev. Lett.* **109**, 266406 (2012).
- [19] H. Gretarsson, J. P. Clancy, X. Liu, J. P. Hill, E. Bozin, Y. Singh, S. Manni, P. Gegenwart, J. Kim, A. H. Said, et al., *Phys. Rev. Lett.* **110**, 076402 (2013).
- [20] I. I. Mazin, H. O. Jeschke, K. Foyevtsova, R. Valentí, and D. I. Khomskii, *Phys. Rev. Lett.* **109**, 197201 (2012).
- [21] K. Foyevtsova, H. O. Jeschke, I. I. Mazin, D. I. Khomskii, and R. Valentí, e-print arXiv:1304.2258v3 (2013).
- [22] G. Chen, R. Pereira, and L. Balents, *Phys. Rev. B* **82**, 174440 (2010).
- [23] L. Binotto, I. Pollini, and G. Spinolo, *Phys. Stat. Sol. (B)* **44**, 245 (1971).
- [24] I. Pollini, *Phys. Rev. B* **53**, 12769 (1996).
- [25] K. Momma and F. Izumi, *J. Appl. Crystallogr.* **44**, 1272 (2011).
- [26] E. V. Stroganov and K. V. Ovchinnikov, *Ser. Fiz. i Khim.* **12**, 152 (1957).
- [27] Y. Kobayashi, T. Okada, K. Asai, M. Katada, H. Sano, and F. Ambe, *Inor. Chem.* **31**, 4570 (1992).
- [28] A. Kuzmenko, *Reffit: Software to fit optical spectra* (<http://optics.unige.ch/alexey/refit.html>, 2014).
- [29] J. M. Fletcher, W. E. Gardner, A. C. Fox, and G. Topping, *J. Chem. Soc. (A)* p. 1038 (1967).
- [30] G. Guizzetti, E. Reguzzoni, and I. Pollini, *Phys. Lett.* **70A**, 34 (1979).
- [31] S. Rojas and G. Spinolo, *Solid State Commun.* **48**, 349 (1983).
- [32] P. Yu and M. Cardona, *Fundamentals of Semiconductors: Physics and Materials Properties* (Springer, New York, 2010).
- [33] T. K. Sham, *J. Am. Chem. Soc.* **105**, 2269 (1983).
- [34] F. M. F. de Groot, Z. W. Hu, M. F. Lopez, G. Kaindl, F. Guillot, and M. Tronc, *J. Chem. Phys.* **101**, 6570 (1994).
- [35] J. P. Clancy, N. Chen, C. Y. Kim, W. F. Chen, K. W. Plumb, B. C. Jeon, T. W. Noh, and Y.-J. Kim, *Phys. Rev. B* **86**, 195131 (2012).
- [36] S. Bhattacharjee, S.-S. Lee, and Y. B. Kim, *New J. Phys.* **14**, 073015 (2012).
- [37] X. Liu, V. M. Katukuri, L. Hozoi, W.-G. Yin, M. P. M. Dean, M. H. Upton, J. Kim, D. Casa, A. Said, T. Gog, et al., *Phys. Rev. Lett.* **109**, 157401 (2012).
- [38] J. Chaloupka, G. Jackeli, and G. Khaliullin, *Phys. Rev. Lett.* **110**, 097204 (2013).
- [39] I. Kimchi and Y.-Z. You, *Phys. Rev. B* **84**, 180407 (2011).
- [40] V. Vijay Shankar et al., unpublished (2014).
- [41] J.-M. Carter and H.-Y. Kee, *Phys. Rev. B* **87**, 014433 (2013).
- [42] J.-M. Carter, V. Shankar V., and H.-Y. Kee, *Phys. Rev. B* **88**, 035111 (2013).
- [43] J. G. Rau, E. K.-H. Lee, and H.-Y. Kee, *Phys. Rev. Lett.* **112**, 077204 (2014).
- [44] Y. Yamaji, Y. Nomura, M. Kurita, R. Arita, and M. Imada, arXiv:1402.1030 (2014).
- [45] V. M. Katukuri, S. Nishimoto, V. Yushankhai, A. Stoyanova, H. Kandpal, S. Choi, R. Coldea, I. Rousochatzakis, L. Hozoi, and J. van den Brink, *New J. Phys.* **16**, 013056 (2014).
- [46] C. Loken, D. Gruner, L. Groer, R. Peltier, N. Bunn, M. Craig, T. Henriques, J. Dempsey, C.-H. Yu, J. Chen, et al., *J. Phys.: Conf. Series* **256**, 012026 (2010).